

DP-MS-78-52
ACC# 735027

RECORDS ADMINISTRATION

AGTH

SRL
RECORD COPY

THE DETECTION AND STUDY OF PLUTONIUM PARTICLES
FOLLOWING THE REPROCESSING OF REACTOR FUEL

S. M. Sanders and A. L. Boni

This document was prepared in conjunction with work accomplished under Contract No. DE-AC09-76SR00001 with the U.S. Department of Energy.

DISCLAIMER

This report was prepared as an account of work sponsored by an agency of the United States Government. Neither the United States Government nor any agency thereof, nor any of their employees, makes any warranty, express or implied, or assumes any legal liability or responsibility for the accuracy, completeness, or usefulness of any information, apparatus, product or process disclosed, or represents that its use would not infringe privately owned rights. Reference herein to any specific commercial product, process or service by trade name, trademark, manufacturer, or otherwise does not necessarily constitute or imply its endorsement, recommendation, or favoring by the United States Government or any agency thereof. The views and opinions of authors expressed herein do not necessarily state or reflect those of the United States Government or any agency thereof.

This report has been reproduced directly from the best available copy.

Available for sale to the public, in paper, from: U.S. Department of Commerce, National Technical Information Service, 5285 Port Royal Road, Springfield, VA 22161, phone: (800) 553-6847, fax: (703) 605-6900, email: orders@ntis.fedworld.gov online ordering: <http://www.ntis.gov/ordering.htm>

Available electronically at <http://www.doe.gov/bridge>

Available for a processing fee to U.S. Department of Energy and its contractors, in paper, from: U.S. Department of Energy, Office of Scientific and Technical Information, P.O. Box 62, Oak Ridge, TN 37831-0062, phone: (865) 576-8401, fax: (865) 576-5728, email: reports@adonis.osti.gov

INTRODUCTION

A program has been in progress at the Savannah River Laboratory to characterize plutonium-bearing particles released to the atmosphere from nuclear fuel reprocessing plants. Nuclear fuel reprocessing facilities at the Savannah River Plant release to the atmosphere minute quantities (< 1 mCi yr) of ^{239}Pu in particulate form. To determine the source, chemical form and physical form of these particles, the initial phase of this program was devoted to the development of collection and analysis techniques for their detection and isolation. Particles bearing plutonium were then identified, isolated from other collected particles, and characterized as to size, morphology, elemental composition, and radioactive properties.

METHODS AND MATERIALS

Particle Collection

Particles are collected by drawing a fraction of exhaust air through membrane filters. These filters are polycarbonate films 47 mm in diameter and 5 μm thick with 5×10^8 0.1- μm diameter pores/cm², giving a filter porosity of 0.024. The filters are supported in a polycarbonate aerosol holder.* Air is drawn through the holder by a small diaphragm pump with a Viton** diaphragm at a rate of four liters per minute to give a face velocity at the filter of 3.8 cm/sec. At this flow, the total efficiency for particle collection by the processes of impaction, diffusion, and interception, calculated according to Spurny,³ is 100% for all particles with diameters of 0.001 μm (the diameter of gas molecules) or larger.

Arrangement of the air sampling system is shown in Figure 1. As particles accumulate on the membrane filters, membrane porosity and air flow are reduced. To determine the fraction of the exhaust sampled, integrated air flow is measured with a dry type test meter† in series with the diaphragm pump. When nitrogen dioxide is present, exhaust gas is passed through two gas drying towers between the filter and the pump. The first tower contains indicating Drierite†† to remove moisture from the air and save the Ascarite††† in the second tower. The self-indicating Ascarite, in turn, absorbs nitrogen dioxide to protect the pump and the dry test meter. A small flowmeter is mounted on the exhaust side of the dry test meter to give an indication of the instantaneous flow rate

* The aerosol holders and membrane filters were produced by Nuclepore Corporation, Pleasanton, California and obtained from them or Bio-Rad Laboratories, Richmond, California.

** Trademark of E. I. du Pont de Nemours & Company, Inc.

† Manufactured by the American Meter Division of Singer.

†† Trademark of W. S. Hammond Drierite Company.

††† Trademark of Arthur H. Thomas Company.

through the system. Air from the meter is fed back into the exhaust system to prevent its release to the service area.

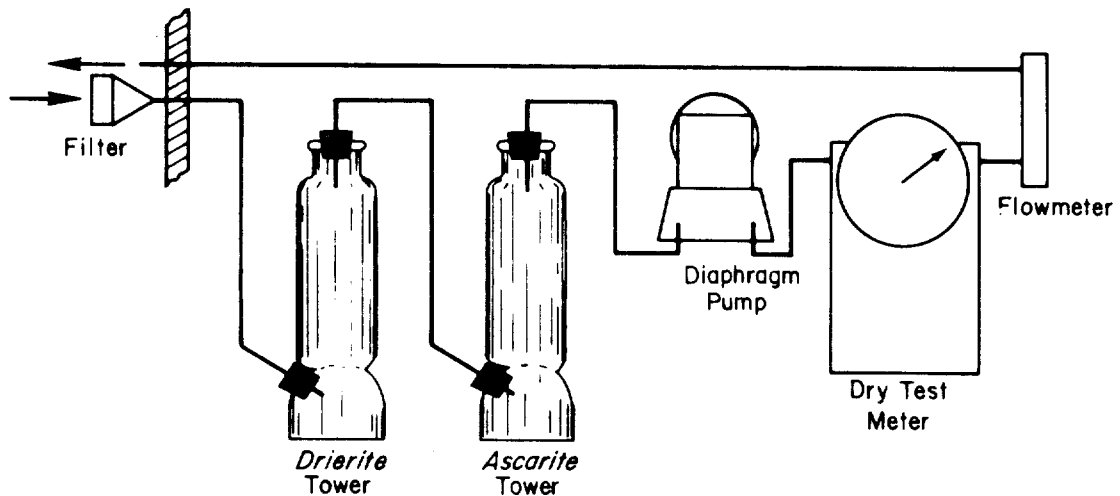


FIGURE 1. Arrangement of Sample Collection Equipment

Film Preparation

Figure 2 shows the procedure for converting the particle-containing filter membrane to a polycarbonate film. After air is sampled, the radioactivity retained on each filter is measured before it is handled in the laboratory. Each filter is then dissolved in a 40% (v/v) solution of 1,2-dichloroethane in dichloromethane. The filters are folded and each placed in a 1-mL volumetric flask. A second clean, unused filter is placed in the same flask to give sufficient polycarbonate to form a 50-mm square film. Volume of the dichloroethane solution in the flask is adjusted to about 3/4 mL. This mixture is stirred until the polycarbonate filters dissolve. The flasks are stoppered and allowed to stand for 30 minutes to allow trapped air bubbles to rise to the surface.

The clear polycarbonate solution containing the particles is poured onto a clean, 50-mm (two-inch) square glass plate (see Figure 2). One edge of a second 50-mm square glass plate is used to spread the solution evenly over the surface of the first plate. The solution is stirred continuously with the second plate for about half a minute while the solution thickens. A 50-mm square, 1.6-mm thick acrylic support with a 45-mm diameter hole is placed on top of the wet film. The support and plate combinations are placed in covered petri dishes for 16 hours while the films continue to dry.

The glass plates are then removed by dipping the support and plate combinations in distilled water and prying the supports from the glass with tweezers.

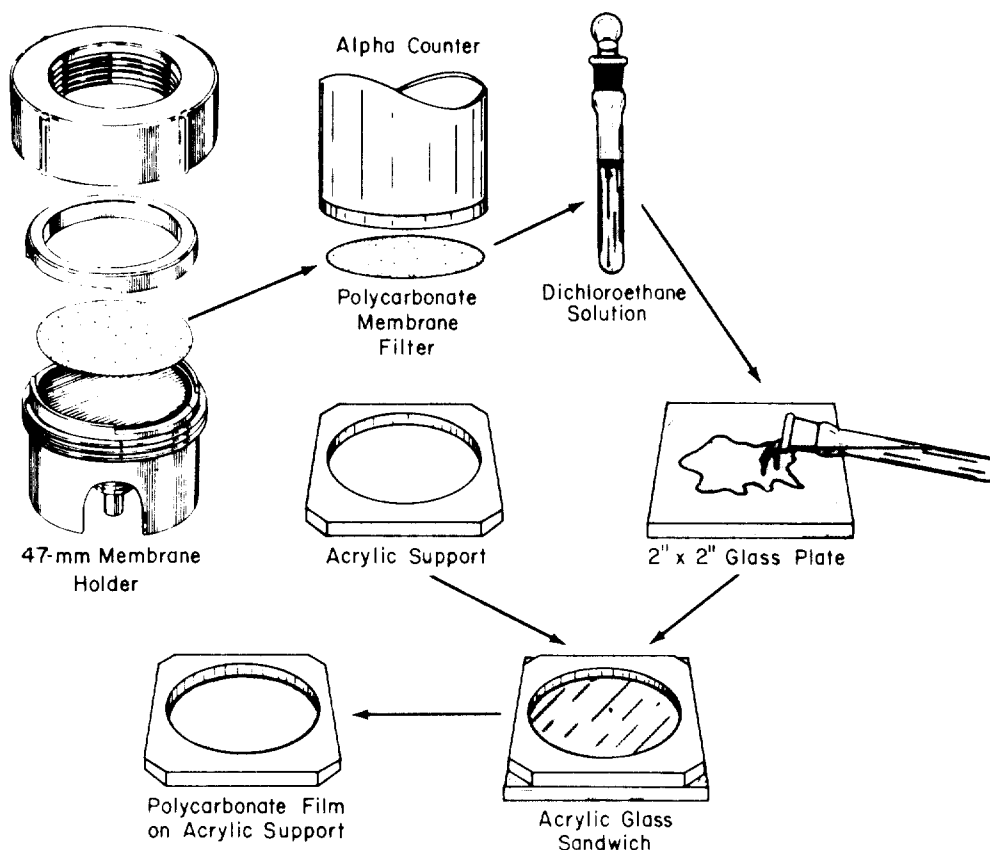


FIGURE 2. Procedure for Preparing Polycarbonate Films

Film Irradiation

To produce fission fragment tracks in the polycarbonate film by which particles containing fissionable material can be identified, the cast film is irradiated in a thermal neutron fluence of about 9×10^{14} neutrons per cm^2 . Films are arranged for irradiation by stacking the supports on top of each other thus sandwiching each film between two supports. Included in the stack are blank films that are prepared in the same way as the sample films from clean unused filters. The assembled stack is wrapped with cellophane tape. Wrapped with each stack are preweighed 25.4-mm diameter, 0.25-mm thick, Type 302 stainless steel disks. The induced radioactivity from 27-day ^{51}Cr in these disks is later measured to determine the thermal neutron fluence to which the particles are exposed.

The packaged stacks are irradiated in a three-inch diameter hole in a light water-cooled, enriched uranium-fueled standard pile with graphite reflectors.⁴ Following irradiation, the induced radioactivity of the stacks are allowed to decay several days before the packaged stacks are returned to the laboratory.

Film Etching

To make the fission fragment tracks visible with an optical microscope, the polycarbonate film is etched for ten minutes in 6N NaOH at 52 to 55°C. During this etching process, a portion of all polycarbonate surfaces is dissolved: the outer surface of the cast film, the surface around the particle, and especially that along the fission fragment tracks.

Emulsion Coating

To identify the fissionable material in each particle, the alpha particle emission rate is measured by coating the polycarbonate film with a photographic emulsion which is developed after a predetermined exposure time.

The emulsion used to coat irradiated films is Kodak Type NTB nuclear-track emulsion (Kodak catalog number 164 4425). Under darkroom lighting (No. 2 Wratten-filtered), a 4-oz jar of emulsion is partly immersed in a water bath maintained at 40°C until the emulsion melts (between 15 and 20 minutes). Slightly over half the molten emulsion is carefully poured into a narrow polyethylene container in the water bath. The molten emulsion is tested by dipping a clean glass microscope slide into it and examining the coat on the glass under a safelight to determine whether bubbles are present. If present, they are scooped from the surface of the molten emulsion with a porcelain spoon.

The polycarbonate films are coated with emulsion by holding the supports containing the films vertically by one corner and dipping them into the clear molten emulsion for about one second. The films are kept vertical until the excess emulsion has drained off. The coated films are then placed horizontally in a biochemical oxygen demand (BOD) incubator maintained at 28°C and about 80% relative humidity until the emulsion cools and gels (about 30 minutes).

Exposure

To determine the alpha particle emission rate for each aerosol particle, the polycarbonate films are stored for one week before being developed. Spun aluminum *Desiccators** containing 60 grams of indicating *Drierite* are used to contain the films during this exposure of the emulsion to the particles. The *Desiccators* are sealed with black adhesive tape and stored in a refrigerator between 4 and 5°C for the duration of the exposure.

* Trademark of Fisher Scientific Company.

Emulsion Processing

At the end of the exposure period, the alpha particle tracks in the emulsion are developed and all substances other than tracks are removed from the emulsion. The emulsion is developed in a 1:1 solution of *Dektol** developer for three minutes at 17°C.^{5,6,7}

Immediately following development, the film is rinsed in 28% (v/v) acetic acid for 10 seconds. The high acid concentration is used to prevent reticulation of the emulsion and its separation from the supporting polycarbonate film.

The rinsed emulsion is fixed by placing it for five minutes in a 1:5 dilution of Kodak rapid fixer concentrate** containing 2.8% (v/v) hardener concentrate.

All chemicals except the metallic silver are washed from the emulsion using a batch process. The emulsion-covered film is placed in distilled water, and the chemicals in the emulsion and wash water are allowed to approach equilibrium for two minutes. The emulsion is then placed in a second container of distilled water while the water in the first container is changed. This process is repeated a total of eight times. After the water wash, the emulsion-coated polycarbonate films are placed in racks and allowed to dry in a dust-free atmosphere.

The entire process is carried out in a dark room where the temperature is maintained between 17 and 18°C. All solutions and the wash water are stored in the dark room so there will be no temperature gradient between solutions during processing.

Track Counting

The film is prepared for track counting by placing the acrylic support on a 50-mm square, 1.6-mm thick acrylic block.

Those particles having tracks are located under a Bausch and Lomb stereo zoom microscope using transmitted light and a magnification of 105X. When found, each particle with tracks is circled with a felt-tip marking pen. After a particle has been marked, the support and block holding the film are moved to a Zeiss photomicroscope where the fission fragment and alpha particle tracks are counted using transmitted light and a magnification of 1000X. Epiplan, flat-field objectives are used because they are corrected for uncovered specimens and do not require cover glasses. The numbers of alpha particle tracks in the lower and upper emulsions are added to give the total number of alpha tracks observed.

Three Polaroid pictures of tracks from a single particle -- one with the focal plane in the lower emulsion, one in the polycarbonate film, and one in the upper emulsion -- are given in Figure 3.

* Trademark of Eastman Kodak Company.

** Kodak Photographic Products catalog numbers 146 4106 or 146 4114.

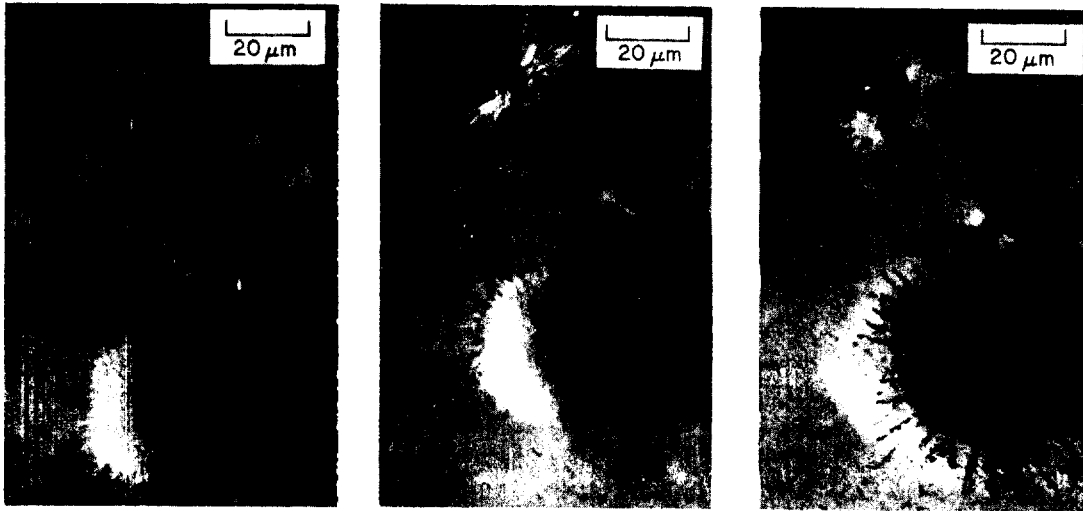


FIGURE 3. Alpha Particle and Fission Fragment Tracks in Photographic Emulsion and Polycarbonate

Identification of Fissionable Materials

Table I gives the theoretical ratios of alpha particle to fission fragment tracks which would be produced from particles irradiated with a fluence of 8.64×10^{14} thermal neutrons/cm² when there is a seven-day interval between film casting and etching and during exposure to nuclear-track emulsion. The stipulation that etching follows film casting by seven days is included because spontaneous fissions will add to the number of fission fragment tracks during this period.

This identification procedure can be used to distinguish particle-bound plutonium from uranium. Table I shows that, of the six isotopic mixtures of uranium, only the highly enriched uranium mixture will give a number of fission fragment tracks comparable to that of the plutonium mixtures. Even if there should be enough uranium to produce fission fragment tracks, mixtures of these isotopes would not produce alpha particle tracks.

This procedure may be used not only to identify plutonium, but also to identify the plutonium isotopic composition in a particle. For example, a particle having 10 fission fragment tracks would also have 5 alpha particle tracks if the mixture were low-irradiation plutonium, 640 alpha particle tracks if it were high-irradiation plutonium, and 5080 alpha particle tracks if it were heat source plutonium.

Table I includes (in addition to U and Pu track data) a number of curium and californium nuclides which could mimic the plutonium mixtures. Some of these nuclides decay by spontaneous fission. To detect spontaneous fissioning, the polycarbonate film should be allowed to stand several weeks after casting and then be etched both before and after thermal neutron irradiation. Under these conditions, tracks due to spontaneous fissioning will appear in unirradiated films.

TABLE I

Theoretical Number of Fission and Alpha Tracks from
 10^{10} Atoms and the Ratio of Alpha to Fission Tracks

<i>Nuclides</i>	<i>Fission Tracks per 10^{10} Atoms</i>	<i>Alpha Tracks per 10^{10} Atoms</i>	<i>Ratio of Alpha to Fission Tracks</i>
Power Reactor Fuel (4% ^{235}U)	3.99×10^2	2.14×10^{-1}	5.36×10^{-4}
Low Burn-Up Uranium (2.5% ^{235}U)	2.50×10^2	1.50×10^{-1}	6.00×10^{-4}
Highly Enriched Uranium (90% ^{235}U)	8.98×10^3	6.54	7.29×10^{-4}
Natural Uranium (99% ^{238}U)	7.18×10^1	5.74×10^{-2}	7.99×10^{-4}
Depleted Uranium (~100% ^{238}U)	2.49×10^1	3.60×10^{-2}	1.44×10^{-3}
High Burn-Up Uranium (1% ^{235}U)	8.88×10^1	1.44×10^{-1}	1.62×10^{-3}
^{247}Cm	1.25×10^3	8.10	6.48×10^{-3}
$^{242\text{m}}\text{Am}$	1.31×10^5	4.20×10^3	3.19×10^{-2}
^{233}U	9.06×10^3	8.20×10^2	9.05×10^{-2}
^{245}Cm	3.73×10^4	1.56×10^4	4.17×10^{-1}
Low-Irradiation Pu (94% ^{239}Pu)	1.20×10^4	(6.48-7.52) $\times 10^3$	(5.40-6.27) $\times 10^{-1}$
^{247}Cm (SF)	<6.64	8.10	>1.22
^{251}Cf	8.30×10^4	1.48×10^5	1.78
^{248}Cm (SF)	5.78×10^1	3.37×10^2	5.84
High-Irradiation Pu (40% ^{239}Pu)	8.02×10^3	(5.13-9.31) $\times 10^4$	(6.40-1.16) $\times 10^1$
^{249}Cf	2.88×10^4	3.79×10^5	1.32×10^1
^{252}Cf (SF)	3.13×10^6	5.02×10^7	1.61×10^1
^{243}Cm	1.19×10^4	4.43×10^6	3.71×10^2
Heat Source Plutonium (80% ^{238}Pu)	2.40×10^3	(1.22-1.07) $\times 10^6$	(5.08-4.46) $\times 10^2$
^{250}Cf (SF)	1.56×10^4	1.02×10^7	6.50×10^2
^{246}Cf (SF)	1.56×10^1	2.76×10^4	1.76×10^3
^{241}Am	5.43×10^1	3.07×10^5	5.66×10^3
^{252}Cf	5.53×10^2	5.02×10^7	9.08×10^4
^{244}Cm (SF)	2.03×10^1	7.34×10^6	3.62×10^5

Measurement of Plutonium and Uranium Ratios

To demonstrate the effectiveness of this identification method in distinguishing between plutonium and uranium, samples of particles were obtained from two sources of known nuclide mixtures: one of low-irradiation plutonium and one of highly enriched uranium. Polycarbonate films were prepared containing particles from either one or the other source. The films were irradiated and coated with emulsion, and the emulsion was exposed and developed using this procedure. The number of alpha particle and fission fragment tracks with each particle were counted.

The data from 315 particles containing low-irradiation plutonium are given in Table II and those from 350 particles containing highly enriched uranium are given in Table III. The data were ranked according to the number of observed fission fragment tracks per particle to determine whether the number of tracks influenced the measured ratios. The mean and standard deviation of the ratios in each track interval are also given.

TABLE II

Analyses of Particles Containing ^{239}Pu

<i>Fission Tracks</i>	<i>Number of Particles</i>	<i>Total Fission Tracks</i>	<i>Total Alpha Tracks</i>	<i>Ratio Alpha to Fission Tracks</i>	<i>Standard Deviation</i>
3-4	33	125	108	0.86	0.68
5-9	80	528	358	0.68	0.49
10-14	65	783	569	0.73	0.44
15-19	36	607	489	0.81	0.45
20-24	26	570	432	0.76	0.38
25-29	11	294	275	0.94	0.50
30-34	13	408	417	1.02	0.38
35-39	7	262	287	1.10	0.32
40-44	16	672	819	1.22	0.44
45-49	9	423	398	0.94	0.45
50-54	4	212	302	1.42	0.72
55-59	1	58	41	0.71	
60-64	0	371	362	0.98	0.30
65-69	2	136	124	0.91	0.08
80-84	2	160	172	1.08	0.46
85-89	1	86	86	1.00	
90-94	2	182	147	0.81	0.18
100-104	<u>1</u>	<u>104</u>	<u>56</u>	<u>0.54</u>	
Total	315	5981	5442	0.91	

TABLE III

Analyses of Particles Containing ^{235}U

<i>Fission Tracks</i>	<i>Number of Particles</i>	<i>Total Fission Tracks</i>	<i>Total Alpha Tracks</i>	<i>Ratio Alpha to Fission Tracks</i>
3-4	124	435	3	0.0069
5-9	146	935	2	0.0021
10-14	39	460	0	0.0000
15-19	18	293	0	0.0000
20-24	10	214	0	0.0000
25-29	3	82	0	0.0000
30-34	4	126	0	0.0000
35-39	3	110	0	0.0000
40-44	3	125	0	0.0000
Total	350	2780	5	0.0018

From Tables II and III the mean ratio (alpha to fission fragment tracks) for low-irradiation plutonium is 9.1×10^{-1} while that for highly enriched uranium is 1.8×10^{-3} . Thus, ^{239}Pu can clearly be distinguished from ^{235}U using this procedure if there is a sufficient number of tracks. However, these ratios are 1.7 and 2.5 times the theoretical ratios given in Table I. In the case of highly enriched uranium, all alpha particle tracks were observed as single tracks only, some of which may have been due to background radiation; this would explain the higher mean ratio for uranium. With plutonium, the higher observed ratios are probably due to the geometry of the media in which the tracks are formed. The polycarbonate film in which the particles are embedded is thin enough for alpha particle tracks to be recorded in the emulsion on both sides. Thus, some of the fission fragments emitted in the vertical direction produce short tracks or no tracks. Likewise, some of the alpha particles emitted in the horizontal direction do not reach the emulsion and give no tracks. If the thickness of the polycarbonate film is less than $2R_\alpha R_f / (R_\alpha + R_f) \approx 2R_\alpha / 3$, where R_α is the range of the alpha particles and R_f is the range of the fission fragments, then the observed ratio will be higher than the theoretical ratio.

There appears to be some influence of the number of tracks counted on the observed ratio. This apparent influence is probably due to the increasing difficulty in counting all the fission fragment tracks with increasing numbers.

Quantitative Radiographic Analysis

Alpha particle and fission fragment track counts will provide not only a ratio from which the fissionable material carried on the particles can be identified, but also an estimate of the quantity of the radioactive nuclides present. One femtocurie (fCi) of ^{239}Pu will produce about 22 alpha particles in a week and, when irradiated with a fluence of 8.64×10^{14} thermal neutrons/cm², will produce about 40 fission fragments. In a mixture of low-irradiation plutonium, the number of fission fragments produced will be increased to 53 with between 28 and 33 alpha particles depending on the age of the mixture. Only about half of these particles will produce tracks, yet this radiographic technique is much more sensitive than electron microprobe analysis, which is not sensitive to less than 10 fCi¹.

Particle Isolation

After a particle has been identified and photographed and the tracks are counted, the particle is excised from the film in a polycarbonate square. For this, the support and block holding the film are returned to the stereo microscope. In transmitted illumination and at a magnification of 105X, two parallel cuts are made through the emulsion-coated film on either side of the particle using an ultramicrotome. The film is then rotated through 90° and two more cuts are made forming a square (see Figure 4a). The cut square is then probed in one corner by a 15-mm long, electrolytically sharpened, tungsten needle (made by placing a pair of 0.52-mm diameter tungsten wires in a 3N NaOH solution and applying a 60-Hz, 10-volt potential between them for 10 to 15 minutes). With this needle, the cut square containing the particle is lifted from the film and placed on a glass microscope slide (see Figures 4b, 4c, and 4d). The polycarbonate square is freed from the needle by rotating it so the corner of the square opposite that stuck by the needle strikes the slide causing the square to rotate and fall.

The emulsion layers are then removed from the polycarbonate square by placing a cover glass on top of the square. Water is introduced between the cover glass and slide using a glass microbrush made from a 20- μL glass disposable pipet. (A 0.025-mm-diameter tungsten wire is doubled and threaded through the lumen forming a loop at one end. A small amount of glass wool is placed through this loop, which is then drawn into the end of the pipet. The glass fibers are then cut off about 2 mm from the end of the pipet.) The microbrush is dipped in water and the glass fibers are touched to the edge of the cover glass to allow the water to flow from the brush to between the slide and the cover glass.

The emulsion is then removed by gently moving the cover glass a few mm from side to side (see Figure 4e); this rolls the swollen emulsion from the surface of the film, but not from the fission fragment tracks themselves. The cover glass is carefully lifted from the glass microscope slide, taking care not to lose the polycarbonate square containing the particle.

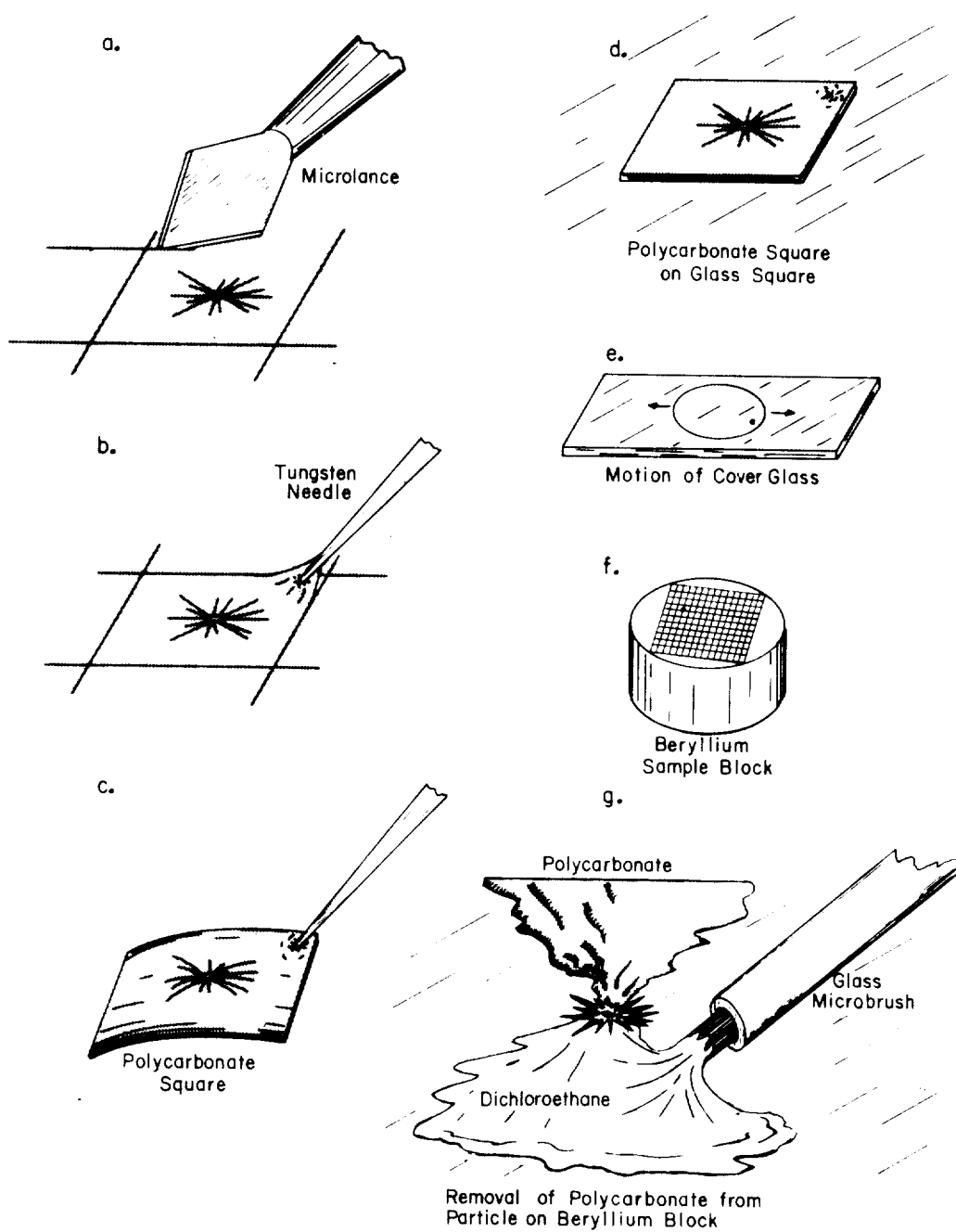


FIGURE 4. Procedure for Mounting Particle for Fissionable Material Identification

Particle Mounting

To mount a particle, the polycarbonate square is placed in a selected grid location on a beryllium sample mounting block* (Figure 4f).

* Walter C. McCrone Associates, Inc. catalog number XIII-403-3.

These sample mounting blocks are 25 mm in diameter and 13 mm thick and fit the standard electron microprobe sample holders, which grip the sides and provide the necessary electrical contact. The top surface of the block is highly polished and contains a grid network of 1-mm squares inscribed on the surface. The squares are numbered in mirror image fashion both vertically and horizontally through the center.

With coaxial (reflected light) illumination and 15X magnification under a stereo microscope, the polycarbonate squares are moved from the microscope slide to the beryllium block using an electrolytically sharpened, tungsten needle.

The polycarbonate square is then dissolved and washed back from the particle using dichloroethane, leaving the particle usually connected to the main body of polycarbonate by a thin isthmus of plastic. This connection does not seriously effect the microprobe analysis and aids in later locating the particles and holding them on the beryllium block. A glass microbrush is rinsed in dichloroethane to remove any foreign material and filled by immersing the bristled end in a second beaker of dichloroethane. The magnification was increased to 105X. Dichloroethane from the brush is dispensed on the beryllium block just in front of the polycarbonate square until the square is engulfed in the solution. The microbrush is then used to push the solution back from the particle. Gelatin replicas of the fission fragment tracks remained with the particles.

The beryllium block is returned to the photomicroscope where a second Polaroid picture of each particle is made at a magnification of 556X to identify the particles after the gelatin has been removed.

The gelatin with each particle is oxidized by exposure to an oxygen plasma for three hours in a low-temperature asher.* In this asher a gas plasma is generated in oxygen using the energy of electrons in the gas. Power is supplied to electrons at 13.56 MHz by a radio-frequency (RF) generator. Since the energy to do this with a low-temperature asher is provided through the electrons instead of heat energy, high temperature degradation, volatilization, or fusion of the inorganic constituents of the particles are eliminated.

Figure 5 illustrates the last three stages in the preparation of one particle. The top picture is the particle in the polycarbonate film with emulsion stripped off. The middle picture is the same particle with the polycarbonate removed showing the gelatin replicas of the fission-fragment tracks. The bottom picture is a scanning electron micrograph of the particle after oxidation of the gelatin. In this picture, traces of the gelatin replicas and silver grains can be seen. Here, what had appeared to be a single particle is actually a conglomeration of at least five and possibly ten smaller particles.

* Manufactured by International Plasma Corporation.

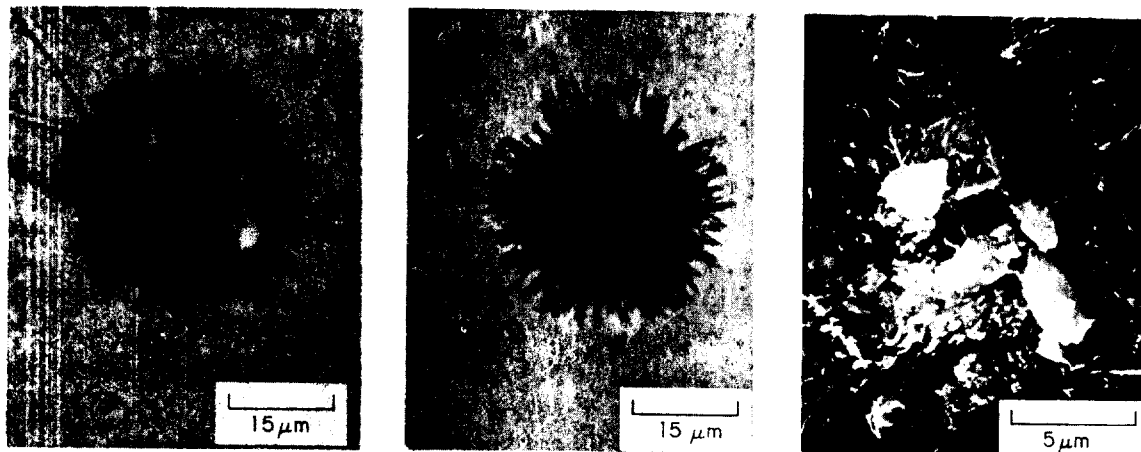


FIGURE 5. Plutonium-Bearing Particle in Last Stages of Mounting

Particle Sizing

To maintain control of particles after the gelatin track replicas are oxidized, the beryllium sample block is returned to the photomicroscope where each particle is located and photographed again under reflected light using Polaroid film and a magnification of 556X. An arrow is marked on the film pointing to the particle, so there will be no mistake in what is intended for analysis.

The size of each particle is estimated from these Polaroid pictures taken after oxidation of the completely denuded particles. An average of the smallest and largest dimensions of the photographed particle are measured in μm and divided by the magnification.

Elemental Analysis

To determine elemental composition of the particles, the particles are analyzed on a Cameca MS46 electron microprobe, equipped with four crystal, wave-length-dispersive spectrometers (take-off angle, 18°) and an *EDAX 701/MICROEDIT** energy-dispersive analyzer. X-ray intensities resulting from the electron bombardment of the particles and particle sizes and shapes are estimated. These estimates, along with estimated average densities, are used in the FRAME program⁸ as modified for particles work by Armstrong⁹ on a *UNIVAC*** 1110 computer. This calculation gives the particle composition in both element and oxide weight percents and atomic proportions based on 24 for oxygen atoms.

* Trademark of EDAX International, Inc.

** Trademark of Sperry Rand Corporation.

SAMPLING LOCATIONS

Particles were collected from air in both exhaust systems in nuclear fuel reprocessing facilities at the Savannah River Plant. A schematic diagram of these systems is given in Figure 6. System I takes room air from inside wet cabinets (where plutonium is in solution) and from work areas and exhausts it via the JB-Line stack.¹ System II takes air from the mechanical line (where plutonium is handled in metallic form) and exhausts it via the 291-F stack. In System I, samples were taken of unfiltered cabinet air from the fifth and sixth levels (Sampling Points 29 and 30, respectively), of filtered air from both locations (Sampling Point 27), and unfiltered room air from the fifth level (Sampling Point 23, and of air at the 156-foot level of JB-Line stack (Sampling Point 28). In System II, samples were taken of mechanical line air from just beyond the first high-efficiency, particulate air (HEPA) filters located in back of the cabinets (Sampling Point A or 31); of the combined air from the mechanical line, air sample exhaust, furnace off-gas vessel vent, process vacuum system, and air dryer system after the second HEPA filter (Sampling Point B or 26); of the air leaving the sand filter which also contained air from the support laboratory off-gas system of Building 772-F, the fuel dissolving and extraction process vessel vent system and Building 221-F canyons containing the process vessels (Sampling Point C); and of air from the 50-foot level in the 291-F stack where air from the sand filter mingles with that from the uranium recovery A-Line and other sources (Sampling Point D).

A total of 121 particles were analyzed from System I (16 from sampling point 23, 68 from point 29, and 38 from point 30) and 417 from System II (125 from sampling point A, 107 from point B, 114 from point C and 71 from point D). These figures do not include 20 particles which contained no elements with atomic numbers greater than 9 and were assumed to be organic.

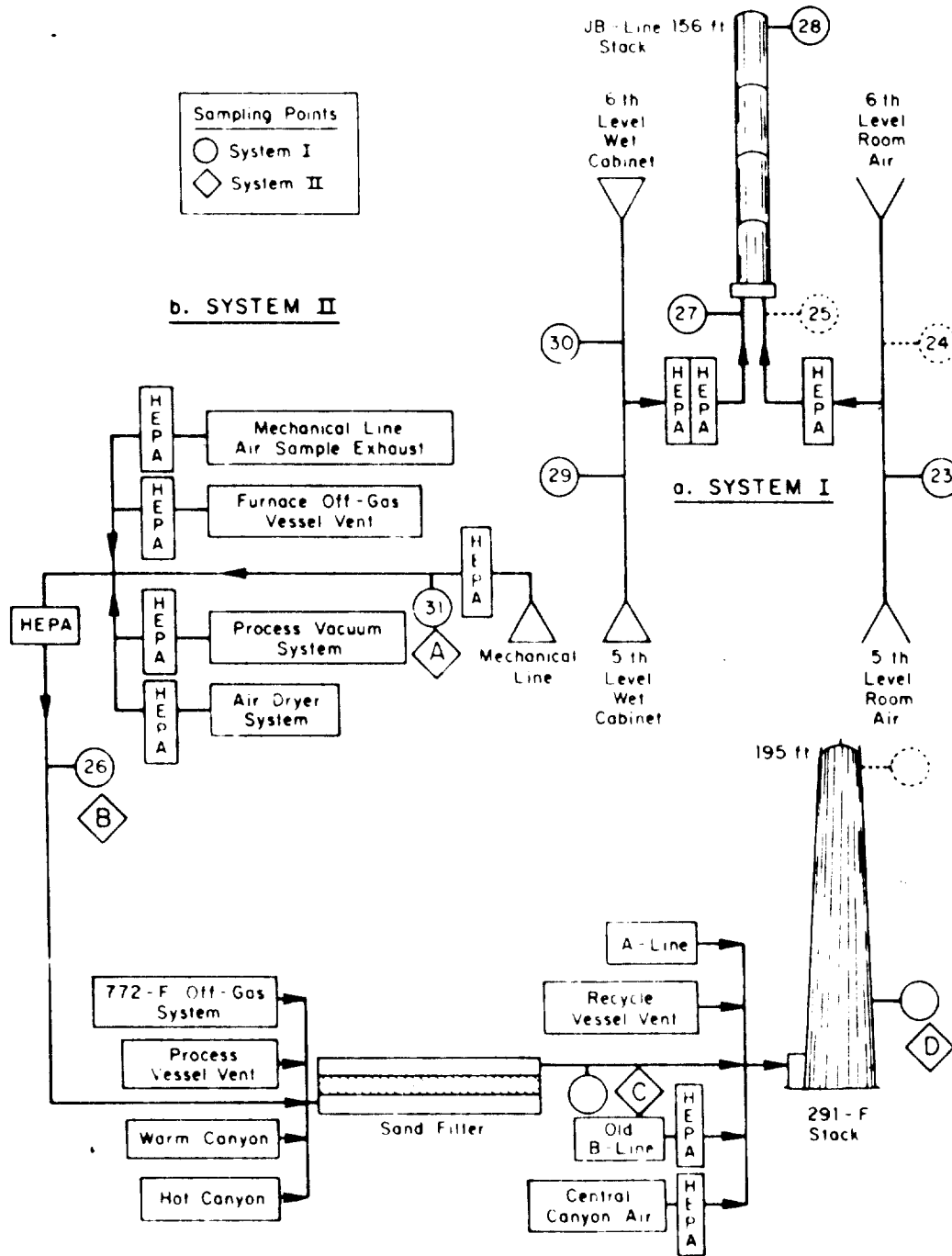


FIGURE 6. Savannah River Nuclear Fuel Reprocessing Facility Exhaust Systems

GROUPING OF DATA BY ENRICHMENT FACTORS

The results were expressed in terms of "enrichment factors" (dimensionless ratios of elemental concentrations), which enabled the intercomparison of the compositions of plutonium-bearing particles with other atmospheric aerosols and the intracomparison among particles collected from different sampling points. A definition of enrichment factors and an explanation of their development and application in this work is given in the Appendix to this report.

To compare the chemical composition of the particles collected from Systems I and II with each other and with the average for global crustal aerosol, the particle analyses were grouped according to the level of the enrichment factors. Four groups were established for each element using the elemental concentration data in Table A-1 of the Appendix. The first group contained those particles which contained no detectable amounts of the element sought. The second group contained detectable amounts with enrichment factors less than one standard deviation below the geometric mean enrichment factor, \overline{EF}_g/s_g . The third group contained particles with enrichment factors between the lower and upper limits of one standard deviation from the geometric mean enrichment factor, \overline{EF}_g/s_g and $\overline{EF}_g \cdot s_g$, respectively. The fourth group contained enrichment factors greater than one standard geometric mean enrichment factor, $\overline{EF}_g \cdot s_g$. The third column of Table IV gives the percent of the particles analyzed which gave positive analyses for each element. The fourth, fifth, and sixth columns of Table IV contain the percent of those having positive analyses which had enrichment factors less than, between, and more than the lower and upper limits of the geometric standard deviation.

To compare the chemical composition of particles collected at the various sample points in System II with each other and global crustal aerosol (Table A-1), this process was repeated and the results are listed in Table V.

Particles having no detectable amounts of an element were not counted with those with enrichment factors less than the lower limit for the geometric standard deviation (s_g) because there can be no zero or negative concentration of enrichment factor values in log-normal frequency distributions. Thus the size of the three groups are expressed as the percent of the particles giving positive analyses, rather than the percent of the total number of particles.

PARTICLE EVALUATION BY SIZE

In this study, particles were selected for analysis based on the number of observed fission-fragment tracks. There being many more particles than could be analyzed, those having three or four tracks were generally passed over in favor of those surrounded by 50 or more tracks. The selection of particles for analysis, however, was not biased by physical size. The size of the particles was

TABLE IV

Comparison of Analyses of Particles from Systems I and II

Element	System	Positive Analyses, %	% of Positive Analyses ^a		
			Less Than ^b	Within ^c	Greater Than ^d
Si	I	100	47	24	29
	II	99	29	30	41
Al	I	84	0	100	0
	II	88	0	100	0
Fe	I	93	14	35	51
	II	79	36	33	31
Ca	I	70	53	30	17
	II	52	41	40	19
Na	I	70	13	72	15
	II	54	8	81	10
K	I	90	56	30	14
	II	63	35	41	24
Mg	I	51	24	59	17
	II	39	38	52	10
Ti	I	74	20	17	65
	II	31	12	13	76
P	II	1	0	17	83
Mn	I	10	0	0	100
	II	12	4	8	88
Ba	II	0.5	0	0	100
S	I	17	47	47	5
	II	70	28	60	13
Cl	I	34	13	67	21
	II	40	2	82	16
Cr	I	53	0	18	82
	II	29	0	9	91
Ni	I	56	2	25	73
	II	9	0	3	97
Zn	I	64	4	41	55
	II	45	5	52	43
Co	II	1	0	0	100
Sc	II	0.2	0	0	100
Cu	I	36	12	37	51
	II	7	6	29	65

TABLE IV CONT'D

W	I	1	0	0	100
	II	0.5	0	0	100
Cd	II	0.2	0	0	100

a. The percent of the positive analyses less than, within, and greater than one geometric standard deviation of the global geometric mean enrichment factor.

b. $EF < \overline{EF}_g / s_g$

c. $\overline{EF}_g / s_g \leq EF \leq \overline{EF}_g \cdot s_g$

d. $EF > \overline{EF}_g \cdot s_g$

TABLE V

Comparison of Analyses of Particles from Sampling Points A, B, C, and D of System II

Element	Sampling Point	Positive Analyses, %	% of Positive Analyses ^a		
			Less Than ^b	Within ^c	Greater Than ^d
Si	A	99	35	33	32
	B	98	8	24	69
	C	100	36	31	33
	D	99	40	31	29
Al	A	79	0	100	0
	B	94	0	100	0
	C	89	0	100	0
	D	96	0	100	0
Fe	A	98	31	22	46
	B	100	40	39	21
	C	58	33	41	26
	D	49	46	34	20
Ca	A	56	20	44	36
	B	77	54	38	9
	C	41	45	40	15
	D	27	53	32	16
Na	A	55	18	60	22
	B	90	4	94	2
	C	39	5	82	14
	D	24	6	94	0
K	A	76	20	48	31
	B	73	46	44	10
	C	55	35	32	33
	D	37	54	27	19
Mg	A	63	33	58	9
	B	48	35	55	10
	C	17	47	42	11
	D	21	60	27	13
Ti	A	42	12	6	83
	B	27	10	24	66
	C	30	14	11	74
	D	15	9	18	73
P	A	2	0	50	50
	C	3	0	0	100
	D	1	0	0	100
Mn	A	7	13	0	88
	B	30	3	9	88
	C	5	0	0	100
	D	6	0	25	75

TABLE V CONT'D

Ba	A	1	0	0	100
	B	1	0	0	100
S	A	58	30	54	17
	B	93	21	69	10
	C	66	24	61	15
	D	61	47	44	9
Cl	A	43	4	47	49
	B	72	1	99	0
	C	27	0	97	3
	D	10	14	86	0
Cr	A	27	0	6	94
	B	58	0	15	85
	C	13	0	0	100
	D	14	0	0	100
Ni	B	27	0	3	97
	C	4	0	0	100
	D	7	0	0	100
Zn	A	53	14	35	51
	B	88	0	69	31
	C	22	4	24	72
	D	6	0	75	25
Co	B	5	0	0	100
Sc	C	1	0	0	100
Cu	A	22	7	33	59
	B	3	0	0	100
	C	1	0	0	100
W	A	1	0	0	100
	B	1	0	0	100
Cd	D	1	0	0	100

a. The percent of the positive analyses less than, within, and greater than one geometric standard deviation of the global geometric mean enrichment factor.

b. $EF < EF_{gms}$

c. $EF_{gms} < EF < EF_{gms}$

d. $EF > EF_{gms}$

not measured until after the particles had been mounted and the polycarbonate film containing the tracks dissolved. Thus the size distribution of the analyzed particles is indicative of the size distribution of particles in the aerosol carrying most of the plutonium.

Cumulative frequency plots were constructed for particles from Systems I and II. Particles in each system were first ranked in order of their approximate diameter in μm from the smallest to the largest. A list of the number of particles having successively larger diameters was made. A cumulative total of the number of particles at increasing diameter segments was calculated and then normalized by dividing by the total number of particles from each system. This gave the fraction of the particles having a diameter equal to or smaller than any particular diameter. Table VI lists the particle diameters in μm ; and, in Columns 2, 3, 4, 5 & 6, the fraction of the particles having diameters equal to or less than each diameter measured in System I and sampling points A, B, C, and D in System II, respectively. These fractions are also plotted on the logarithmic probability graph given in Figure 7.

TABLE VI

Comparison of Size Distributions of Particles from System I and II with Natural Aerosols¹

Diameter (D), μm	Fraction with Diameter $\leq D$					
	System I	Sampling Point A	Sampling Point B	Sampling Point C	Sampling Point D	Natural Aerosol
0.4	0.03			0.01	0.01	
0.5	0.04			0.02		
0.9	0.07			0.04	0.06	
1.1				0.09	0.08	0.25
1.2				0.10		0.42
1.4				0.11		0.64
1.7				0.14	0.11	
1.8	0.28	0.02		0.17		0.83
2.2	0.30			0.32	0.21	0.91
2.5				0.34	0.23	
2.7	0.35	0.04	0.01	0.37	0.24	0.949
3.0				0.42	0.31	
3.3				0.43	0.32	
3.6	0.53	0.10	0.06	0.46	0.34	0.979
3.9		0.11				0.983
4.0			0.07	0.51	0.38	
4.4				0.52	0.41	
4.5	0.54	0.13	0.10			0.989
5.0			0.11	0.55	0.48	
5.4	0.62	0.20	0.18	0.60		0.994
5.8			0.20	0.59		
6.1			0.22	0.61	0.56	
6.3		0.23	0.26			0.996
6.7			0.27	0.64	0.58	
7.0				0.67		
7.2	0.67	0.33	0.35	0.68		0.997
7.4				0.68		
7.8			0.36	0.70		
8.0	0.68	0.34	0.37	0.71	0.59	0.998
8.6			0.39		0.63	
9.0	0.75	0.40	0.46	0.74	0.69	0.999
10.0		0.41	0.48	0.78	0.75	
10.8	0.79	0.44	0.60	0.81		
11.7		0.46	0.61	0.82	0.79	
12.6	0.83	0.54	0.62	0.83	0.80	1.000
13.5		0.55	0.66		0.82	
14.4	0.84	0.58		0.89		
14.9			0.67		0.83	
16.2	0.88	0.61	0.71			
17.1		0.62		0.89	0.89	

18.0	0.92	0.64	0.75	0.90	
20.7		0.70	0.81	0.91	0.92
21.6	0.93	0.71	0.82		
23.4		0.74	0.85	0.930	0.930
24.3		0.75	0.86		
25.2	0.94	0.78	0.87		0.972
26.9	0.95	0.81	0.91	0.939	
27.9		0.83	0.92		
28.8			0.93	0.956	0.986
30.6		0.86	0.935		
31.5		0.87		0.974	
32.4		0.88	0.944		
33.5		0.89	0.963		
34.2	0.959	0.94	0.972	0.982	
35.1				1.000	1.000
36.0	0.975	0.944	0.981		
39.6		0.968	0.991		
41.4	0.983		1.000		
50.4	0.992				
53.9		0.992			
59.4	1.000				
62.9		1.000			

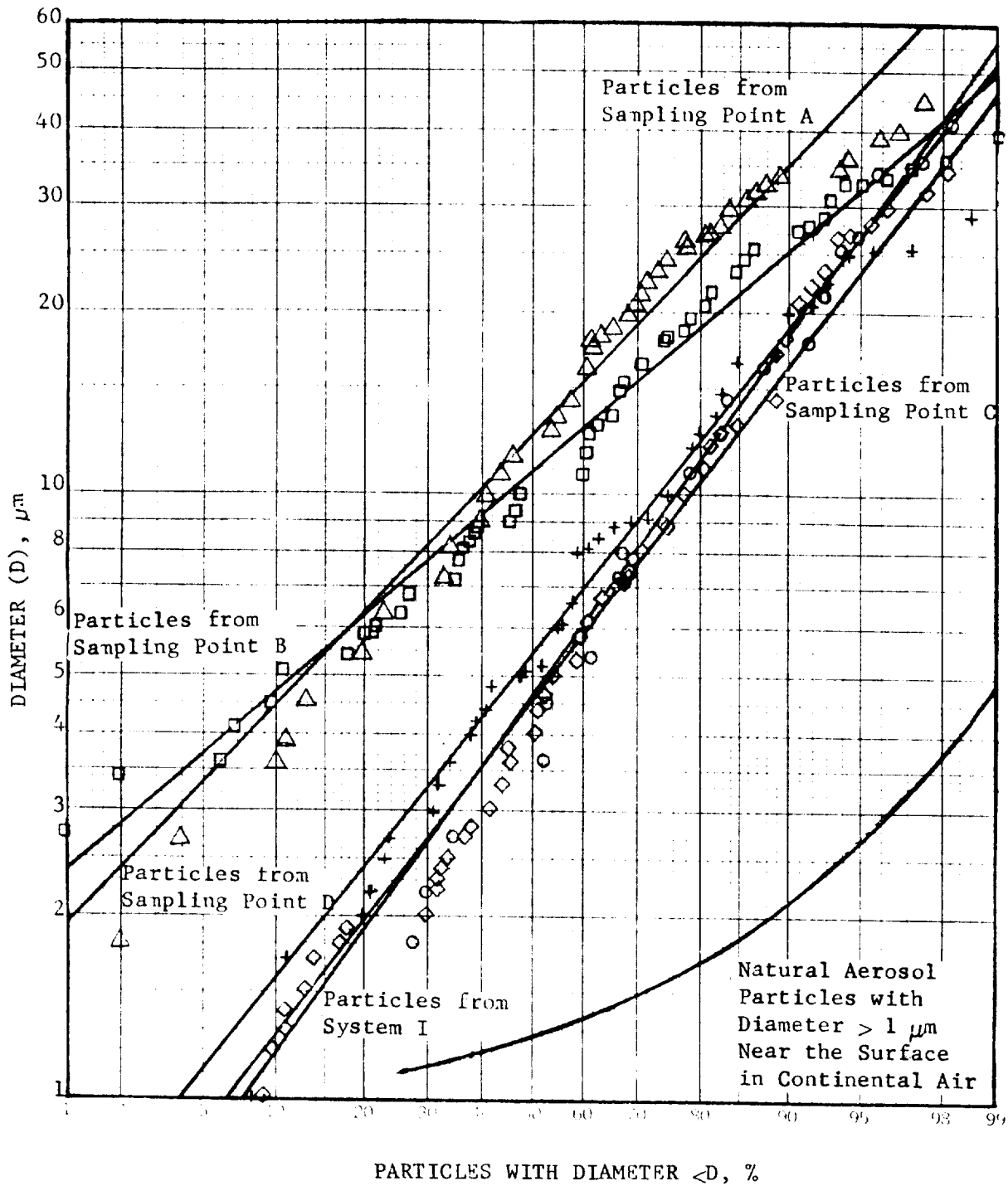


FIGURE 7. Size Distribution Plots for Natural and Collected Particles

For comparison, a cumulative frequency plot was also made of the size distribution of particles in natural atmospheric aerosols. A very simple function that has been used extensively in atmospheric research to express particle size distribution in both natural and polluted atmospheres is

$$\frac{dN}{dD} = aD^{-b} \quad (1)$$

where N is the number concentration or total number of particles per unit volume having diameters from the lower limit of definition of aerosols up to diameter D in μm . From the relationships

$$dD = D d(\ln D) \quad (2)$$

and

$$\ln D = \ln 10 \cdot \log D \quad (3)$$

the more useful expression

$$\frac{dN}{d(\log D)} = (\ln 10)aD^{-c} \quad (4)$$

is obtained where $c = b - 1$, and $dN/d(\log D)$ is called the number distribution. Junge¹⁰ found c to be about 3 over the size range $-0.7 < \log D < 1.5$ or $0.2 < D < 32 \mu\text{m}$. Integrating the first equation between D_0 and D ($D_0 < D$) gives

$$N = \left[\frac{aD^{-c}}{c} \right]_{D_0}^D = \frac{a}{3} \left[\frac{1}{D_0^3} - \frac{1}{D^3} \right] \quad (5)$$

Instead of expressing the distribution as the number of particles per unit volume, it can be expressed as a fraction, F, of the total number of particles or

$$F = \frac{N}{N_T} = 1 - \left[\frac{D_0}{D} \right]^3 \quad (6)$$

where N_T is the total number of particles when $D = \infty$, and $N_T = a/3D_0^3$. To obtain a reasonable distribution, only those particles which could be easily seen with an optical microscope were included. Thus D_0 was assumed to be $1 \mu\text{m}$, and Equation 6 can be expressed as

$$F = 1 - \frac{1}{D^3} \quad (7)$$

The frequency distribution for natural aerosols with particle diameters between 1 μm and D, calculated from this expression, is given in Column 7 of Table VI and plotted in Figure 7.

To see how closely the distribution of particle diameters resembles a log-normal distribution, the assumption was made that the observed diameters represent a sample of a population having a log-normal distribution. The geometric mean diameter, \bar{D}_g , and geometric standard deviation, s_g , were calculated from these data using equations similar to those given earlier for the geometric mean enrichment factor and geometric standard deviation. These values are given in Table VII. Values for the upper 68.27% limit for the diameters were calculated from the product of \bar{D}_g and s_g . The best fit log-normal probability curves were plotted on the logarithmic probability graph in Figure 7 by drawing straight lines through coordinates for \bar{D}_g and $\bar{D}_g \cdot s_g$ on the 50.00 and 84.14* cumulative percent abscissae, respectively.

To determine the degree of asymmetry, the skewness (SK) of these frequency distributions was calculated using the relationship

$$SK = 3 \left(\frac{\ln \bar{D}_g - \ln D_{\text{med}}}{\ln s_g} \right) \quad (8)$$

where D_{med} = the median diameter. A perfect log-normal distribution has a skewness of zero. If a distribution has a higher tail to the right than to the left, it is positively skewed.

TABLE VII

Distribution of Particle Diameters in Systems I and II

System	Sample Location	Data Points N	Geom. Mean Diameter \bar{D}_g	Geom. Std. Deviation s_g	Skewness SK
I		121	4.64	2.92	0.71
II	A	125	12.27	2.24	0.04
II	B	107	10.82	1.93	0.34
II	C	114	4.48	2.75	0.37
II	D	71	5.43	2.69	0.23

* $50.00 + \frac{68.27}{2}$

PARTICLE EVALUATION BY PLUTONIUM CONTENT

Another characteristic studied was the distribution of plutonium among the particles as indicated by the observed number of fission-fragment tracks in the surrounding polycarbonate.

The track distribution among particles from both systems was evaluated in the same way as the particle diameters. The fraction of the particles with the number of tracks equal to or less than a selected number, T , are given for Sampling Points A, B, and D in Table VIII. Figure 8 is a logarithmic probability plot of cumulative percent of particles from each of these sampling points. Figure 9 is a similar plot for particles from four locations in System I. The calculated geometric mean for the number of fission-fragment tracks per particle, the geometric standard deviation, and the skewness for particles from each sampling point are given in Table 9. Best fit log-normal probability curves for each distribution are plotted in Figures 8 and 9. For comparison of the track distributions for particles from the various sampling points in System I with those from System II, the probability curve for the track distribution for particles from Sampling Point A in System II is plotted with the distributions from System I in Figure 9.

TABLE VIII

Distribution of Fission Tracks among Plutonium-Bearing Particles Collected from Sampling Points A, B, C, and D

Number of Tracks	Fraction with Tracks $\leq T$			
	Sample Point A	Sample Point B	Sample Point C	Sample Point D
1	0.04			
2	0.05			
3	0.09			
4	0.13			0.01
5	0.15		0.06	0.03
6	0.19	0.01	0.09	
7	0.21		0.11	
8	0.26		0.13	0.06
9	0.31	0.03	0.15	0.10
10	0.34	0.04	0.20	0.13
11	0.36		0.24	0.21
12	0.38		0.26	0.25
13	0.40	0.05	0.32	0.28
14	0.44	0.07	0.38	0.32
15	0.45	0.07	0.44	0.42
16	0.47	0.08	0.48	0.46
17	0.50	0.11	0.49	0.58
18	0.51	0.15	0.54	0.63
19	0.54	0.17	0.56	0.69
20	0.59	0.21	0.59	0.70
21	0.60	0.22	0.63	0.72
22	0.63	0.26	0.66	0.75
23	0.64	0.31	0.70	0.77
24	0.68	0.37	0.72	0.82
25	0.70		0.75	
26	0.72	0.39	0.78	
27	0.74	0.40	0.82	
28	0.75	0.44	0.87	0.83
29	0.76	0.45	0.89	0.85
30	0.78	0.48	0.90	0.86
31	0.79	0.50	0.92	0.89
32	0.81	0.52	0.93	
33	0.82	0.56	0.947	0.92
34	0.84	0.58		0.93
35	0.85	0.59		0.944
36	0.86	0.60	0.956	
37		0.61	0.965	0.958
38	0.87	0.62		
39	0.88			
40	0.89	0.63		0.972

41		0.65	
42	0.90	0.66	
43		0.68	
44	0.91	0.69	
46	0.91		
47		0.73	
48	0.92	0.75	
49	0.93	0.76	
50	0.945	0.77	0.986
51	0.950		
52		0.78	
54	0.955		0.991
55		0.80	
57		0.81	
58		0.84	
59		0.85	
60	0.960	0.89	
63		0.90	
65			1.000
68		0.91	
70		0.92	
72	0.965		
73		0.93	
75	0.970		
80	0.980	0.93	1.000
82		0.953	
84		0.972	
98		0.981	
100	0.990	0.991	
150	0.995	1.000	
200	1.000		

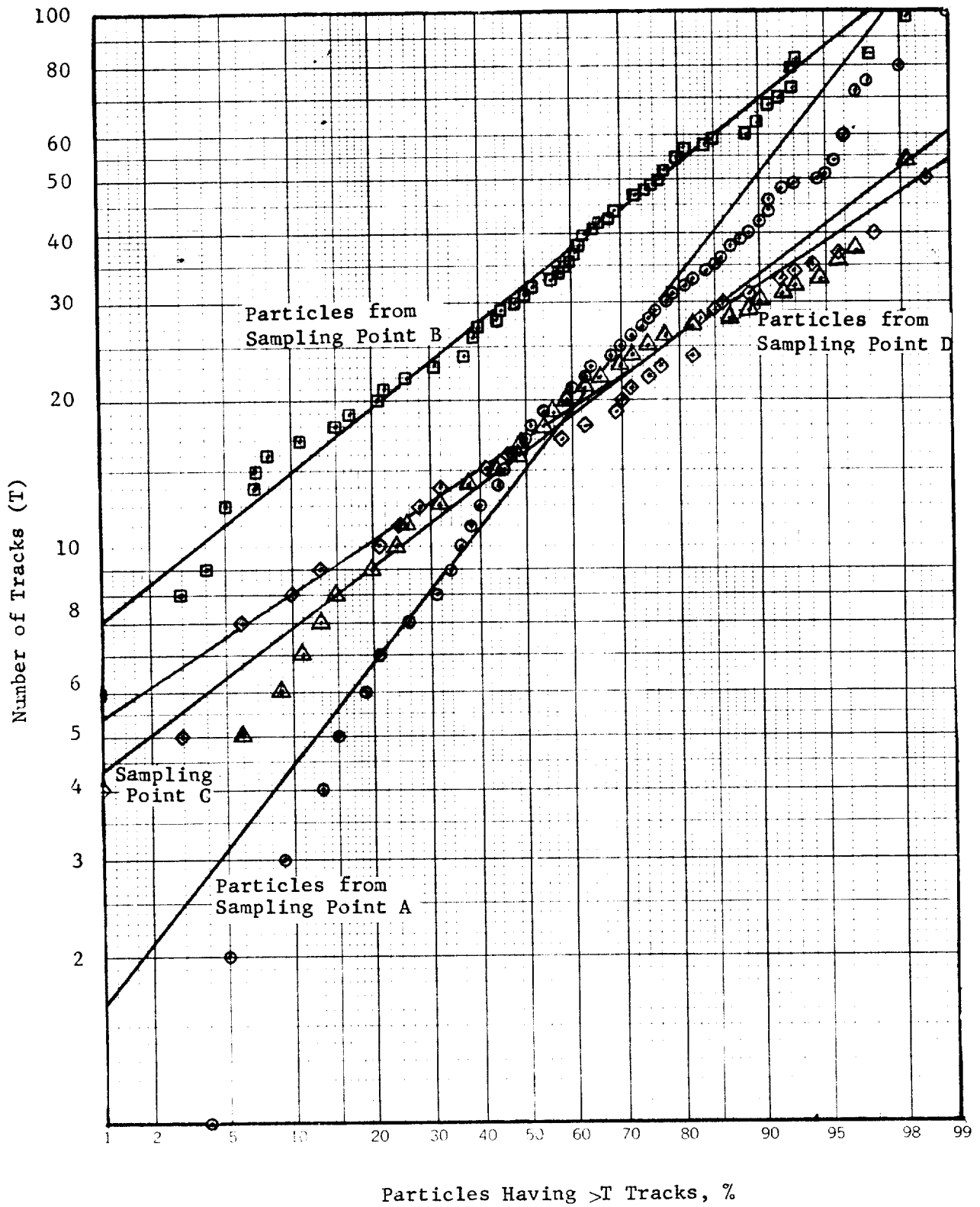


FIGURE 6. Distribution of the Number of Tracks Per Particle for Particles Collected from Sampling Point A, B, C. and D in System II

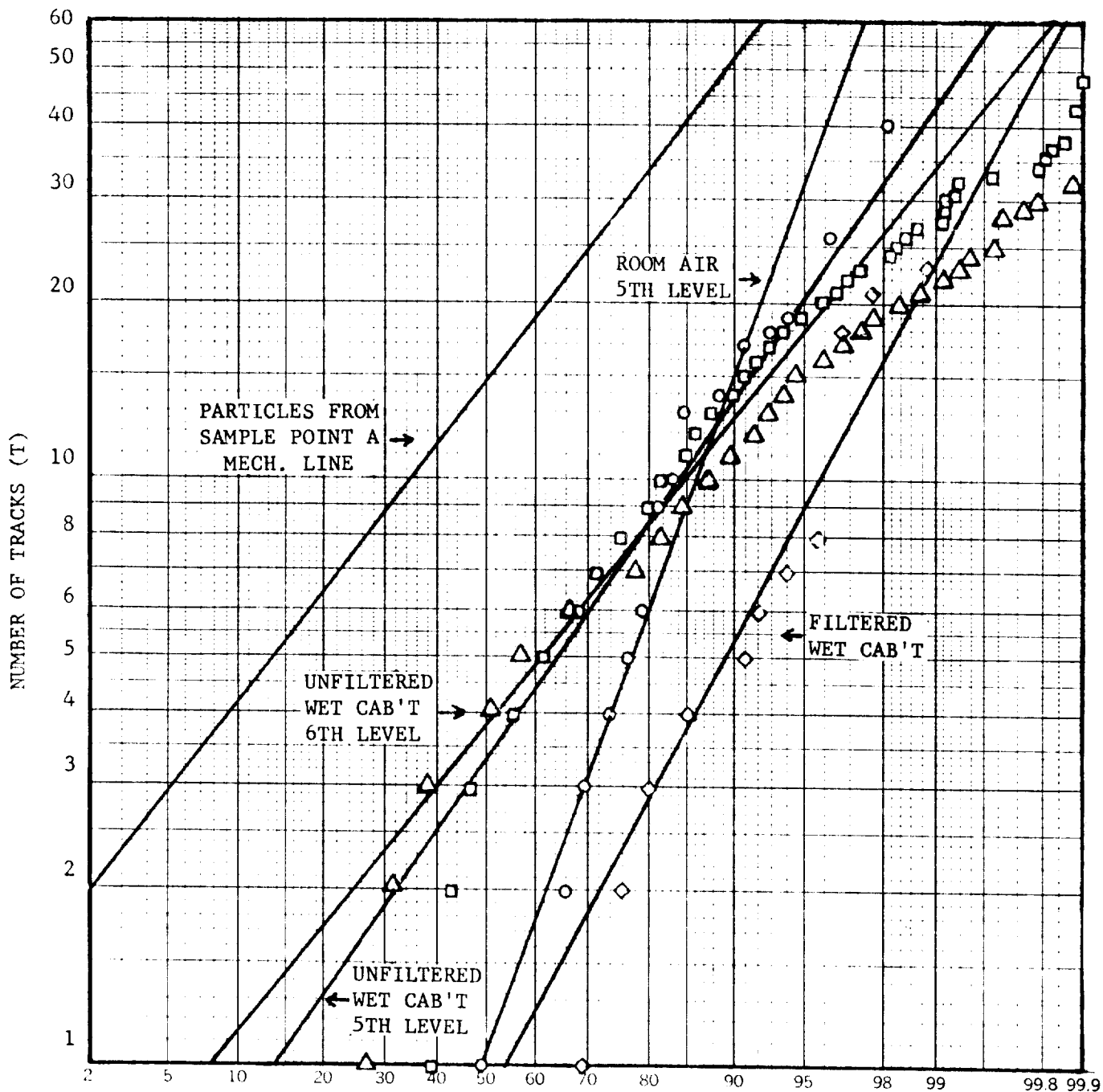


FIGURE 9 . Distribution of the Number of Tracks per Particle for Particles Collected from the Mechanical Line (Sampling Point A) in System I Compared to Particles Collected From Wet Cabinets and Room Air in System II.

TABLE IX

Distribution of Fission Tracks among Plutonium-Bearing Particles from Various Sources in Systems I and II

Source	Data Points, N	Geom. Mean of No. of Fission Tracks, \bar{T}_g	Geom. Std. Deviation, s_g	Skewness, SK
<u>System I</u>				
Unfiltered 5th Level Wet-Cabinet Air	15,987	3.76	2.56	-0.20
Unfiltered 6th Level Wet-Cabinet Air	7,042	3.32	2.99	-0.51
5th Level Room Air ^a	53	1.00	8.40	-0.98
Filtered Wet-Cabinet Air ^a	98	0.87	4.14	-0.29
<u>System II</u>				
Sampling Point A Air	200	14.74	2.69	-0.43
Sampling Point B Air	107	32.38	1.78	0.23
Sampling Point C Air	114	16.50	1.75	-0.22
Sampling Point D Air	71	17.01	1.65	0.24

a. Values determined graphically.

The most abundant elements in average crustal rock (and soil) are oxygen (46.60%), silicon (27.72%), aluminum (8.13%), iron (5.00%), calcium (3.63%), sodium (2.83%), potassium (2.59%), magnesium (2.09%), and titanium (0.44%).⁵ With the exception of oxygen, which was not detected by electron microprobe analyses, these elements are also found in most inorganic particles (Tables I and A-1). This supports the idea that most plutonium-bearing particles are airborne crustal material to which minute quantities of plutonium have become attached.

Of particular interest is the quantity of ^{239}Pu contained on these particles. One femtocurie (1 fCi = 10^{-15} Ci) of ^{239}Pu irradiated under the conditions described here should produce 41 fission-fragment tracks. The minimum detection limit for electron microprobe analysis of plutonium is about 0.2 picograms or about 10 fCi of ^{239}Pu ,¹ which is equivalent to 410 fission-fragment tracks. Because of this relatively low sensitivity of electron microprobe analysis, plutonium could be detected by this method in only one of the 558 particles selected for analysis, even through all the particles produced fission-fragment tracks. This single particle was a small, 1- μm -diameter particle, collected from unfiltered wet-cabinet exhaust. It contained 73% PuO_2 by weight (equivalent to 170 fCi of ^{239}Pu) in combination with Fe_2O_3 and mica.

Of the major crustal elements listed in Table IV, silicon and iron were the most ubiquitous being found in most particles. The enrichment factor distribution for these elements, however, does not fall within the log-normal distribution for crustal material. For the enrichment factors of an element to match the log-normal distribution of crustal material in aerosols, there should be about 16% of the enrichment factors of less than one geometric standard deviation, 68% within one geometric standard deviation of the mean, and another 16% above one geometric standard deviation. This lack of conformity may result from the low values for the geometric standard deviations of the enrichment factors for these elements in aerosols.

Only the enrichment factors for sodium and chlorine fall within the log-normal distribution for crustal material. This may be due to the relative high solubility of compounds of these elements and, in the case of chlorine, the high value for the geometric standard deviation.

Particles from System I contain a greater variety of elements than those from System II and thus all but four elements are contained on higher proportion of particles from System I than from System II. The most striking example was nickel. While 56% of the particles from System I contained nickel, only 9% of those in System II did. The major crustal elements (those in Table A-1 comprising 0.4% or more of crustal material) are contained on over half the particles from System I and with the exception of magnesium in particles from sampling points C and D and titanium are also contained on over half the particles from System II. Some of the minor elements (those comprising 0.1% or less of crustal material) are present in over half the particles, viz, nickel, chromium, and zinc in particles from System I and sulfur, chromium, and zinc in particles from sampling point B of System II. The chromium and nickel may have come from the 304L stainless steel alloy of cabinets and exhaust ducts or the Hastelloy*-C alloy in the wet cabinets. However, few of the particles contained the proper ratio of chromium-to-nickel found in either alloy. Also, if Hastelloy-C contributed the nickel in the particles, some molybdenum should also have been detected.

* Trademark of Cabot Corporation, Boston, Mass.

Of the elements which are present on less than 10% of the particles, all but copper on particles from System II have high enrichment factors. This indicates that the minor constituents of crustal material are not uniformly distributed among particles but are concentrated on a few particles where they represent a major constituent.

The plutonium-bearing particles were larger than natural aerosol particles collected at relatively low altitude (<2.3 km) as seen in Figure 7. Those particles collected from sampling points A and B of System II were larger than those from System I, with geometric mean diameters two or three times those of particles from other locations.

The size of about 95% of the plutonium-bearing particles range between 0.4 and 37 μm in diameter which lies in the range that will be deposited in the lungs. Morrow¹⁸ estimates that with normal respiration, all particles in a monodispersed aerosol of unit density spheres 37 μm in diameter will be deposited in the nasopharyngeal region of the respiratory tract. With larger (>37 mm) particles, the fraction deposited rapidly decreases. As the diameter decreases, the fraction deposited in the lungs decreases until a minimum of 20% deposition is reached for particles around 0.1 to 0.2 μm in diameter where the particles tend to remain airborne. As the diameters decrease below 37 μm , a larger fraction is deposited in the tracheobronchial region, until 70% of the particles 5 μm in diameter are deposited in the tracheobronchial region and only 5% in the nasopharyngeal and 5% in the alveolar regions. With still smaller particles, the fraction deposited in the tracheobronchial region decreases until at 0.2 μm diameter only 10% are deposited in the tracheobronchial and 10% in the alveolar regions. For dust particles having a density of around 2.5, this distribution will be shifted toward smaller diameters so that 100% deposition occurs around 5 μm .

Particles from all parts of System II also contained on the average more plutonium per particle than those from System I. As seen in Table IX, the geometric mean number of tracks per particle from unfiltered wet-cabinet air was just over three for both fifth- and sixth-level cabinets (averaging about 0.08 fCi per particle), while that for filtered wet-cabinet air was about one-third of this or almost the same for room air (averaging about 0.02 fCi/particle).

A comparison of the mean diameters of particles collected from different sampling points, given in Table VII, with the mean number of fission fragment tracks for particles from the same location, given in Table IX, indicate a possible relationship between particle size and plutonium content. Correlation coefficients between the cube of the particle diameter and the number of fission fragment tracks from each particle from sampling points B, C, and D were calculated. These are given in Table X. These coefficients differ significantly from that expected from a random sample from a population of paired variables having a correlation coefficient of zero. Thus, even though the points on a plot of particle diameter cubed versus number of fission fragment tracks appears scattered, there is a significant correlation between the quantity of plutonium in particles collected from sampling points B, C, and D in System II and the particle volume. (Tracks with particles

TABLE X

Correlation Coefficient and Coefficient of Alienation for the Cube of the Diameter and the Number of Fission Fragment Tracks for Particles From Sampling Points B, C, and D of System II.

Sanpling Point	Number of Particles	Correlation Coefficient
B	107	0.69
C	114	0.29
D	71	0.36

collected at other sampling points, where only ^{239}Pu could be found, were counted but not recorded for each particle. Only where a ratio of alpha particle to fission fragment tracks was needed to distinguish plutonium bearing particles from those having other fissionable materials were the track counts recorded).

APPENDIX: Use of Elemental Enrichment Factors to Express Particle Compositions

BACKGROUND

Two recent developments in aerosol studies have provided valuable tools for the analysis of particle composition data. The first is the use of ratios of elemental concentrations called "enrichment factors" to compare aerosol compositions. Begun in the early seventies, this technique has gained wide acceptance in the last few years¹²⁻¹⁶. The second development is the availability of data on the composition of natural aerosols. In the last few months, Rahn² published a compilation of 104 data sets of trace elements in aerosols along with the geometric mean and geometric standard deviation of the enrichment factors for each of the elements. These data sets were from sampling sites ranging from highly industrialized temperate zones to the tropics and poles, and represent all continents except South America, as well as various marine locations. As a framework from which to view much of the order in atmospheric aerosols, Rahn used the concept of aerosol-crust enrichment factors for the elements. This concept has been applied to analyzing data collected in this study to provide for (a) the intercomparison of the compositions of plutonium-bearing particles with atmospheric aerosols compiled by Rahn and (b) the intracomparison among particles collected from different sampling points.

MICROPROBE ANALYSES OF PARTICLES

To be comparable, results of microprobe analyses must be expressed as elemental ratios. The reason for this is that not all elements which may be present in an aerosol are detected by microprobe analysis. The microprobe used in this study is quantitative only for elements with atomic numbers greater than 10. It is only semi-quantitative for oxygen (the most abundant element in crustal material) as well as other major elements of low atomic number such as hydrogen, fluorine, and carbon. Atmospheric aerosols are known to contain, in addition to elements and oxides, carbonaceous material such as sooty carbon and organics and water-soluble ionic material such as sulfate, nitrate, and ammonium ions. Thus elemental weight percents, normalized to 100 based on the elements detected cannot be compared. Even the addition of a hypothetical oxygen concentration, calculated on the supposition that all elements are present as oxides of

known valence, will still not account for the organic fraction of particles. However, a ratio of the concentrations of one element to another will normally be relatively unaffected by the concentrations of other elements which may be present and thus can be used for comparisons even when a complete analysis of all the elements in an aerosol or single particle is not available.

ENRICHMENT FACTORS

A dimensionless ratio of elemental concentrations, called the enrichment factor, has been defined as

$$EF(X) = \frac{(X/Ref)_{\text{aerosol}}}{(X/Ref)_{\text{source}}} \quad (A-1)$$

where $EF(X)$ is the enrichment factor of element X in an aerosol relative to some source material. X/Ref is the ratio of the concentration of element X to the concentration of the reference element, Ref , in both the aerosol and the source material.

SOURCE MATERIAL

Elemental ratios in aerosols or in single particles are normalized by dividing them by ratios of the same elements in a standard source material to obtain the enrichment factors. If a particle is composed of the same material as the source, the enrichment factor will be 1.00 for all elements. If the ratio of an element to the reference element is greater or less than the same ratio in the source material, the enrichment factors will be greater or less than 1.00, and the particle is said to be either enriched or depleted, respectively, in that element.

The most commonly-used crustal source material for continental enrichment-factor calculations is globally-averaged crustal rock. (For marine enrichment-factor calculations, sea salt is used.) The selection of rock may seem strange for there is little doubt that soil rather than rock is the precursor to the crustal aerosol. Some 93% of the earth's continental surface is covered by soil.¹⁷ Many of these soils are in states of loose aggregation which can easily be made airborne by the wind. Chemically, however, Rahn¹² has found that the composition of the crustal aerosol is not unambiguously that of soil. Elements in natural aerosols with rock-like enrichment factors include Si, Fe, Ca, K, and Cr; those with soil-like enrichment factors are Ti and Ba. One would expect natural aerosols to be, like soil, depleted in the more soluble elements. Except for glacial activity and to a lesser extent in deserts, physical weathering processes, which ultimately produce

small particles from boulders, are very slow and are accompanied at all stages by intense chemical weathering. Thus large masses of physically pulverized rock which have not been chemically weathered are not available for aerosol production.

Rahn¹² speculates that remote continental aerosols are never as depleted in the soluble elements (e.g., Na, K, Ca, and Mg) as they should be relative to rock (if natural aerosols were purely soil-derived) because of the presence of small amounts of marine aerosol. Soluble elements, especially Na and Mg, are abundant in the marine aerosol, thus only small amounts of this aerosol in remote continental areas would noticeably raise the proportions of soluble elements in an aerosol collected there.

In addition to the similarity in the elemental composition of aerosol and crustal rock, available analytical data are much less numerous and less reliable for soils, especially for several interesting trace elements which are enriched in aerosols.

For these reasons, the majority of authors who calculate aerosol-crust enrichment factors have chosen one of the several available tables of elemental abundances in average crustal rock. Because the composition of plutonium-bearing particles are compared with data reported by Rahn,¹² the same crustal-rock composition used by him (that reported by Mason¹¹) was selected as the source material composition for this work. Column 2 of Table A-1 gives the elemental concentrations in globally-averaged crustal rock for those elements found in plutonium-bearing particles.

REFERENCE ELEMENT

Of the various elements which seem to be reliably crust-derived in aerosols, aluminum, silicon, and iron are generally considered to be the most suitable reference elements. (When sea salt is the source material, the nearly universal choice is sodium.) An acceptable crustal reference element should have high concentrations in rock and soil, very low pollution potential, ease of determination by a number of analytical techniques, and freedom from contamination during sampling. Iron has markedly higher pollution potential than does aluminum, and so is less suited for use with urban or rural aerosols. Silicon is probably the most unambiguous elemental indicator of crustal material. Unfortunately, silicon has been determined in so few aerosol samples that it can not be used as the reference element where comparisons are to be made. Aluminum is a major element (81,300 ppm in rock), well-determined by a variety of analytical techniques, and has a minimum of specific pollution sources.

TABLE A-1

Elemental Concentrations in Average Crustal Rock and Geometric Mean Enrichment Factors of Various Aerosols

Element	Conc., ppm	<i>Geometric Mean Enrichment Factors</i>					
		<i>Global</i> \overline{EF}_{g/s_y}	<i>Global</i> \overline{EF}_g	<i>Global</i> $\overline{EF}_{g \cdot s_y}$	<i>Remote</i> <i>Marine</i> \overline{EF}_g	<i>Remote</i> <i>Conti-</i> <i>nenal</i> \overline{EF}_g	<i>Urban</i> \overline{EF}_g
Si	277,200	0.62	0.79	1.01	0.7	0.7	0.79
Al	81,300	1.00	1.00	1.00	1.0	1.0	1.00
Fe	50,000	1.05	2.06	4.06	2.5	1.5	2.2
Ca	36,000	1.15	2.84	7.04	8	1.5	2.9
Na	28,300	0.64	4.44	30.8	10^2-10^3	0.4	1.81
K	25,900	0.99	1.98	3.98	6	1.5	1.63
Mg	20,900	0.64	2.38	8.90	10^1-10^2	0.7	2.0
Ti	4,400	1.01	1.39	1.92	1.2	1.2	1.63
P	1,050	0.79	2.63	8.71	-	-	2.6
Mn	950	1.45	3.91	10.5	3	2	3.2
Ba	425	2.61	5.50	11.6	-	~2	4.8
S	260	228	608	1620	-	-	490
Cl	130	100	740	5470	10^4-10^5	40	300
Cr	100	2.50	8.11	26.3	20	6	6.2
Ni	75	8.74	31.9	116	100	50	10.8
Zn	70	79.7	257	832	400	80	300
Co	25	0.91	3.52	13.6	4	1.5	4.6
Sc	22	0.59	1.17	2.34	0.8	0.8	0.60
Cu	55	34.0	102	304	150	20	149
U	1.8	0.92	2.87	8.93	-	-	2.87
W	1.5	4.89	19.1	74.3	-	-	11.0
Cd	0.2	274	1920	13400	5000	2000	940

Thus for this work, enrichment factors for element X in most particles were calculated using

$$EF(X) = \frac{(X/Al)_{\text{particle}}}{(X/Al)_{\text{rock}}} \quad (A-2)$$

with aluminum as the reference element and average crustal rock as the source material. However, 18 particles from System I and 37 from System II contained no aluminum. Thus the enrichment factors had to be based on silicon rather than aluminum where

$$EF(X) = \frac{(X/Si)_{\text{particle}}}{(X/Si)_{\text{rock}}} \cdot \frac{(\overline{Si}/Al)_{\text{g aerosol}}}{(Si/Al)_{\text{rock}}} = 0.79 \frac{(X/Si)_{\text{particle}}}{(X/Si)_{\text{rock}}} \quad (A-3)$$

(The second set of ratios is the geometric mean of the global aerosol-crust enrichment factor explained in the next section.)

Using these two relationships, the enrichment factors were calculated from the elemental weight percents obtained for 115 particles in System I and 156 particles in System II. Six small (0.5 to 3.6 μm diameter) iron particles in System I and two particles ($\sim 15 \mu\text{m}$ diameter containing K, Cr, and Fe [1:3:3]) from Sample Point A of System II contained neither aluminum nor silicon and were thus not included in the study.

COMPARATIVE AEROSOL DATA

To compare the elemental composition of plutonium-bearing particles with that of atmospheric aerosols, enrichment factors calculated for elements in these particles were grouped according to data supplied by Rahn⁶ for aerosols. In his report, trace element concentrations in aerosols from 104 published and unpublished data sets were used to calculate enrichment factors. From the enrichment factors in each data set, the geometric mean enrichment factor (\overline{EF}_g) and geometric standard deviation (s_g) of the logarithmic frequency distributions of enrichment factors were calculated for each element using the following formulae:

$$\overline{EF}_g = \exp \left[\frac{1}{N} \sum_{i=1}^N \ln EF_i \right] \quad (A-4)$$

and

$$s_g = \exp \left\{ \left[\frac{1}{N-1} \sum_{i=1}^N (\ln EF_i - \ln \bar{EF}_g)^2 \right]^{1/2} \right\}$$

where N = the number of data points

EF_i = the enrichment factor of the i th point

The geometric mean enrichment factors obtained by Rahr^{1,2} for 19 elements are given in Table A-1 for global, remote marine, remote continental, and urban aerosols. The geometric means of the global aerosol enrichment factors include data from all points and may be weighted too heavily toward cities, but they can serve as a useful first approximation to a general aerosol. The urban enrichment factors are geometric means for 29 cities. The enrichment factors for remote continental and remote marine areas were read from the enrichment-factor plots and are therefore somewhat subjective.

To obtain the lower and upper limits for 68.27% of the enrichment factors closest to the geometric mean, values for \bar{EF}_g/s_g and $\bar{EF}_g \cdot s_g$, respectively, were calculated using global values. (When describing concentrations at selected statistical levels remote from a mean, the s_g is a multiplier or divider of the \bar{EF}_g , whereas its counterpart Gaussian standard deviation functions as an increment to the arithmetic mean. This is a consequence of the fact that multiplying and dividing values is equivalent to adding and subtracting their logarithms.) The results from these calculations are also given in Table A-1.

REFERENCES

1. S. Marshall Sanders, Jr. *Composition of Airborne Plutonium-Bearing Particles from a Plutonium Finishing Operation*. USERDA Report DP-1445, E. I. du Pont de Nemours and Co., Savannah River Laboratory, Aiken, South Carolina (November 1976).
2. S. Marshall Sanders, Jr. *Characterization of Airborne Plutonium-Bearing Particles from a Nuclear Fuel Reprocessing Plant*. USERDA Report DP-1470, E. I. du Pont de Nemours and Co., Savannah River Laboratory, Aiken, South Carolina (September 1977).
3. Kvetoslav R. Spurny, James P. Lodge, Jr., Evelyn R. Frank, and David C. Sheesley. "Aerosol Filtration by Means of Nuclepore Filters: Structural and Filtration Properties." *Environ. Sci. Technol.* 3 (5), 453-464 (1969).
4. R. C. Axtmann, L. A. Heinrich, R. C. Robinson, O. A. Towler, and J. W. Wade. *Initial Operation of the Standard Pile*. USAEC Report DP-32, E. I. du Pont de Nemours and Co., Savannah River Laboratory, Aiken, South Carolina (1953).
5. *Kodak Materials for Nuclear Physics and Autoradiography*. Kodak Technical Pamphlet No. P-64, Professional and Finishing Markets Division, Eastman Kodak Company, Rochester, New York (1976).
6. George A. Boyd. *Autoradiography in Biology and Medicine*. Academic Press Inc., New York (1955).
7. Beatrix Markus Kopriwa and C. P. Leblond. "Improvements in the Coating Technique of Radioautography." *J. Histochem. Cytochem.* 10 (3), 269 (1962).
8. H. Yakowitz, R. L. Myklebust, and K. F. J. Heinrich. *FRAME: An On-Line Correction Procedure for Quantitative Electron Probe Microanalysis*. National Bureau of Standards Technical Note 796, National Bureau of Standards, Washington, DC (1973).
9. John T. Armstrong and Peter R. Buseck. "Quantitative Chemical Analysis of Individual Microparticles Using the Electron Microprobe: Theoretical." *Anal. Chem.* 47, 2178-2192 (1975).

10. C. E. Junge. *Handbook of Geophysics and Space Environments*. pp. 5-23. S. L. Valley, editor. Air Force Cambridge Research Laboratories, Office of Aerospace Research, US Air Force, Cambridge, Mass. (1965).
11. B. Mason. *Principles of Geochemistry*, 3rd ed., p 45. John Wiley and Sons, New York, N. Y. (1966).
12. Kenneth A. Rahn. *The Chemical Composition of the Atmospheric Aerosol*. Technical Report, Graduate School of Oceanography, University of Rhode Island, Kingston, R.I. (1976).
13. Kenneth A. Rahn. *Sources of Trace Elements in Aerosols - An Approach to Clean Air*. Ph.D. Thesis, University of Michigan, Ann Arbor, Mich. (1971). Xerox University Microfilms (Order No. 72-4956).
14. William H. Zoller, E. S. Gladney, and Robert A. Duce. "Atmospheric Concentrations and Sources of Trace Metals at the South Pole." *Science* 183, 198 (1974).
15. Robert A. Duce, Gerald L. Hoffman, and William H. Zoller. "Atmospheric Trace Metals at Remote Northern and Southern Hemisphere Sites: Pollution or Natural?" *Science* 187, 59 (1975).
16. H. E. Neustadter, J. S. Fordyce, and R. B. King. "Elemental Composition of Airborne Particulates and Source Identification: Data Analysis Techniques." *Air Pollution Control Assoc.* 26 (11), 1079 (1976).
17. E. L. Kothny. "The Three-Phase Equilibrium of Mercury in Nature." *Trace Elements in the Environment*, pp. 48-80. *Advances in Chemistry Series 123*, American Chemical Society, Washington, D. C. (1973).
18. P. E. Morrow. "Evaluation of Inhalation Hazards Based Upon the Respirable Dust Concept and the Philosophy and Application of Selective Sampling." *Amer. Ind. Hygiene Assoc. J.* 25 (2) 213 (1964).